Experimental characterization and modeling of affinity membrane
Proceedings of European Congress of Chemical Engineering (ECCE-6)
Copenhagen, 16-20 September 2007

Experimental characterization and modeling of affinity membrane

J. Labanda, J. Llorens*

Department of Chemical Engineering, University of Barcelona, Martí i Franquès 1, 08028 -Barcelona, Spain
e-mail: jllorensl@ub.edu

Abstract

The present study proposes a model to explain the adsorption process through ion-exchange membrane adsorbers. The model is defined by the continuity equation, expressed as a differential mass balance of the solute over a section of the membrane, and the Langmuir isotherm. The proposed model uses dimensionless variables that were defined by characteristic times of the global process. To examine the validity of the model, the adsorption of an anionic dye (Orange G) through the ion-exchange membrane adsorbers was investigated as a function of dye and KCl concentration, obtaining strong correlation between fitted and experimental breakthrough curves.

Keywords: membrane chromatography, ion-exchange membrane adsorbers, dynamic adsorption, breakthrough curve, anionic dye

1. Introduction

Adsorption and ion-exchange processes are by far the most widely used techniques for high-resolution separation and analysis of dyes. These processes are traditionally carried out using packed beds, which have several major limitations. The pressure drop across a packed bed is generally high. Another major limitation with conventional adsorption and ion-exchange processes is the dependence on intra-particle diffusion for the transport of solute molecules to their binding sites within the pores of such media (Lewus *et al*., 1999; Skidmore *et al*., 1990). This increases the process time since transport of macromolecules by diffusion is slow, and particularly so when it is hindered. Consequently, the recovery liquid volume needed for elution also increases. Some of these factors and the fact that the transport phenomenon is complicated make scale-up of packed bed adsorption and ion-exchange processes difficult.

Recently, a new technology in membrane separation, the membrane chromatography has proven its efficiency and time stability. Membrane chromatography has been studied as an alternative to conventional resin-based adsorption columns for the isolation and purification of molecules. Membrane chromatography combines the advantages of conventional chromatography columns in terms of separation power and capacity with membrane technology regarding mass transfer, high throughput and robustness. The main advantage is the absence of long diffusive paths, thus a process performed with membrane adsorbers is definitely faster than with a traditional column configuration (Boi *et al*., 2006). Hence, membrane chromatography operates in convective mode, which can significantly reduce diffusion and pressure drop limitations commonly encountered in column separation processes (Guo *et al*., 2003). However, diffusive transport is not totally absent.

Membrane chromatography is performed by four types of membrane adsorbers: ion-exchange, affinity, hydrophobic interaction and reversed-phase. The uses of ion-exchange and affinity interactions are more widely reported in the literature (Ghosh, 2002). Affinity membranes has attached onto the membrane surface different ligands that are able to immobilize specific molecules, such as proteins and biomolecules (Lan *et al*., 2001). For example, dyes can function as an ion-exchange to bind proteins by electrostatic interactions (Zhang *et al*., 2002; Arica *et al*., 2004). Nevertheless, ion-exchange membranes retain directly charged molecules and their ion-exchange capacity is given by the introduction to the solid phase of different charged groups such as sulfonic acid, sulfopropyl, diethylaminoethul and quaternarium ammonium. Ion-exchange membranes have been also used for the purification of biomolecules (Knudsen *et al*., 2001).

The aim of the present study was to analyze and model the dynamic adsorption of dye anion with two sulphonic groups in a commercial flat-sheet ion-exchange membrane in respond to the dye concentration and ionic strength changes.

2. Theory

The model is based on a differential mass balance of the solute over a section of the membrane, which is characterized by the surface area, *A*, the thickness, *L*, and the porosity, ε, and the adsorption isotherm of the solute onto the membrane. The model describes the movement of the solute in the membrane adsorber by: (1) time derivation of solute concentration in the liquid-phase, (2) the axial convective flux, (3) axial solute dispersion defined following the Fick's law in the liquid-phase, and (4) the solute adsorption onto the porous surface of the solid-phase as a function of time. Thus, it is defined the following equation:

$$\varepsilon \cdot \frac{\partial c}{\partial t} + \varepsilon \cdot v \cdot \frac{\partial c}{\partial z} = \varepsilon \cdot D \cdot \frac{\partial^2 c}{\partial z^2} - (1-\varepsilon) \cdot \frac{\partial c_s}{\partial t} \qquad (1)$$

where c is the solute concentration in the liquid-phase, c_s is the adsorbed solute concentration in the solid-phase, D is the axial diffusion coefficient and v axial velocity.

Therefore, the adsorption process between the solute and adsorbent can be described by the second order kinetic reversible equation:

$$\frac{\partial c_s}{\partial t} = k_a \cdot c \cdot (c_s^* - c_s) - k_d \cdot c_s \qquad (2)$$

where c_s^* is the maximum adsorbed solute concentration in the solid phase, k_a and k_d are the adsorption and desorption rate constants, respectively.

For a liquid-phase concentration, c, the equilibrium solute concentration in the solid phase, c_{s_eq}, can be deduced by doing $(\partial c/\partial t)=0$ and the Langmuir isotherm appears:

$$c_{s\_eq} = \frac{b \cdot c_s^* \cdot c_{eq}}{1 + b \cdot c_{eq}} \qquad (3)$$

where c_{eq} is the equilibrium solute concentration in the liquid-phase and b is the ratio between the adsorption and desorption rate constants, $b = k_a/k_d$.

To solve the model Eq. (1-3) must be considered with the following initial conditions:

$$c = 0 \quad at \quad z \geq 0, t = 0 \qquad (4)$$

$$c_s = 0 \quad at \quad z \geq 0, t = 0 \qquad (5)$$

and the boundary conditions:

$$\varepsilon \cdot v \cdot c - \varepsilon \cdot D \frac{\partial c}{\partial z} = \varepsilon \cdot v \cdot c_o \quad at \quad z = 0, t > 0 \qquad (6)$$

$$\frac{\partial c}{\partial z} = 0 \quad at \quad z = L, t > 0 \qquad (7)$$

The total solute mass transfer from the liquid-phase to the solid-phase is controlled by four time dependent processes, which can be defined by characteristic times: $t_{process}$ is the average time taken by a liquid element to pass through the membrane, $t_{process} = L/v$, and t_{disp}, t_{ads} and t_{des} are characteristic times related to axial dispersion, adsorption and desorption processes, respectively. The main rate-limiting process will be the process with lower characteristic time value. These three characteristic times permit to define three dimensionless constants as follow:

$$Pe = \frac{t_{disp}}{t_{process}} = \frac{v \cdot L}{D} \qquad (8)$$

$$K_{ads} = \frac{t_{process}}{t_{ads}} = \frac{k_a \cdot c_o \cdot L}{v} \qquad (9)$$

$$r = \frac{t_{des}}{t_{ads}} = \frac{k_a}{k_d} \cdot c_o \qquad (10)$$

where Pe is the axial Peclet number, K_{ads} is the dimensionless adsorption constant and r is ratio between adsorption and desorption constants.
Eq. (1) can be rewritten by introducing the concept of characteristic times as follows:

$$\frac{\partial C}{\partial \tau}+\frac{\partial C}{\partial \zeta}=\frac{1}{Pe}\cdot\frac{\partial^2 C}{\partial \zeta^2}-m\cdot\frac{\partial C_s}{\partial \tau} \quad (11)$$

where C is the ratio between the current and feed solute concentration in the liquid-phase, $C=c/c_o$, C_s is the ratio between the current and equilibrium feed solute concentration in the solid-phase, $C_s=c_s/c_{s\_eq\_o}$, ζ is the dimensionless coordinate along the membrane, $\zeta=z/L$, and τ is the dimensionless time defined as the ratio of current time and the characteristic time of the process, $\tau=t/t_{process}$.

The kinetic isotherm dimensionless equations are rewritten as:

$$\frac{\partial C_s}{\partial \tau}=K_{ads}\cdot\left(C+\frac{1}{r}\right)\cdot\left(C_{s\_eq}-C_s\right) \quad (12)$$

$$C_{s\_eq}=\frac{\frac{r}{p}\cdot C_{eq}}{1+r\cdot C_{eq}} \quad (13)$$

Eqs. (11), (12) and (13) depend also on the following dimensionless variables:

$$C_s=c_s/c_{s\_eq\_o} \quad (14)$$

$$C_{eq}=c_{eq}/c_o \quad (15)$$

$$c_{s\_eq\_o}=(r/(1+r))\cdot c_s^* \quad (16)$$

$$m=\frac{1-\varepsilon}{\varepsilon}\cdot\frac{c_{s\_eq\_o}}{c_o} \quad (17)$$

$$p=\frac{c_{s\_eq\_o}}{c_s^*} \quad (18)$$

The corresponding initial and boundary conditions are:

$$C=0 \quad at \quad \zeta\geq 0,\ \tau=0 \quad (19)$$

$$C_s=0 \quad at \quad \zeta\geq 0,\ \tau=0 \quad (20)$$

$$C-\frac{1}{Pe}\frac{\partial C}{\partial \zeta}=C_o \quad at \quad \zeta=0,\ \tau>0 \quad (21)$$

$$\frac{\partial C}{\partial \zeta}=0 \quad at \quad \zeta=1,\ \tau>0 \quad (22)$$

The model is governed by Eqs. (11), (12) and (13), which were implemented in the program “Mathematica” (Wolfram Research) in order to solve the differentials. As a result, the dynamic adsorption, represented by the breakthrough curve, of a solute through the membrane adsorber can be simulated and compared to experimental data.

3. Experimental

The adsorption of an anionic dye through an ion-exchange membrane adsorber was investigated to evaluate the model predictions. The membrane was supplied by Sartorius (Sartobind S) and it was formed by 3 flat-sheets of anion exchange. The features of this membrane are: approximately 15 cm^2 of membrane area, 25 mm of membrane diameter and the average membrane thickness was assumed to be 0.8 mm. The anionic dye (Orange G) studied was supplied by Aldrich, which is an azo synthetic dye with the following features: Color Index Number = 16230, MW = 452.37 g/mol, λ_{max} = 478 nm.

The anionic dye feed solutions were prepared by mixing the powder dye with a buffer solution at pH = 7 and at three different KCl concentrations (0.1, 0.5 and 1 M). The buffer solution was made by adding 305 mL of 0.2 M in $Na_2HPO_4 \cdot 12H_2O$ and 195 mL of 0.2 M in $NaH_2PO_4 \cdot H_2O$ into 1 L deionized water, and the amount of KCl used depended on the salt concentration needed in the experiment: 7.455, 37.275 and 74.55 grams for adsorption tests and 74.55 grams for desorption test or membrane generation.

Feed solutions were infused in the membrane cartridge by a continuous cycle syringe pump (NE-1000 Multi-PhaserTM from New Era Pump Systems Inc.) set at a constant flow of 1 mL/min. The dye concentrations were determined using a UV-visible spectrophotometer (SECOMAM). All experiments were conducted at a constant temperature, 25 ± 1 ºC.

4. Results and discussion

The breakthrough curves (dimensionless solute concentration versus dimensionless time), which were obtained on the membrane adsorber for various Orange G and KCl feed concentrations, are comparatively given in Figure 1. Lines correspond to the theoretical data calculated by the model commented above. Both the shape of the breakthrough curves and the maximum adsorbed solute concentration in the solid-phase values reveal the relatively poor interaction tendency of the membrane towards Orange G at high KCl feed concentrations, which results in relatively low bindings. The effect of KCl concentrations is more evident at lower Orange G feed concentrations.

The affinity between the solute and membrane comes determined by the increase of solute loaded concentration, thus the affinity is raised when the maximum plateau is reached within a very short time period. For 0.1 M KCl, the dimensionless time needed increase the solute effluent concentration from 0 to 0.95 is 2620, 148 and 52 for the solute feed concentrations of 10^{-3}, $5 \cdot 10^{-4}$ and $2.5 \cdot 10^{-4}$ M, respectively. Therefore, the affinity decreases with decreasing the KCl feed concentration.

The comparison between the theoretical predictions and the experimental data is shown in Figure 1. Small deviations of the breakthrough curves between the model predictions and experimental data are observed. These deviations may be due to the non-ideal membrane adsorber by the presence dead volume.

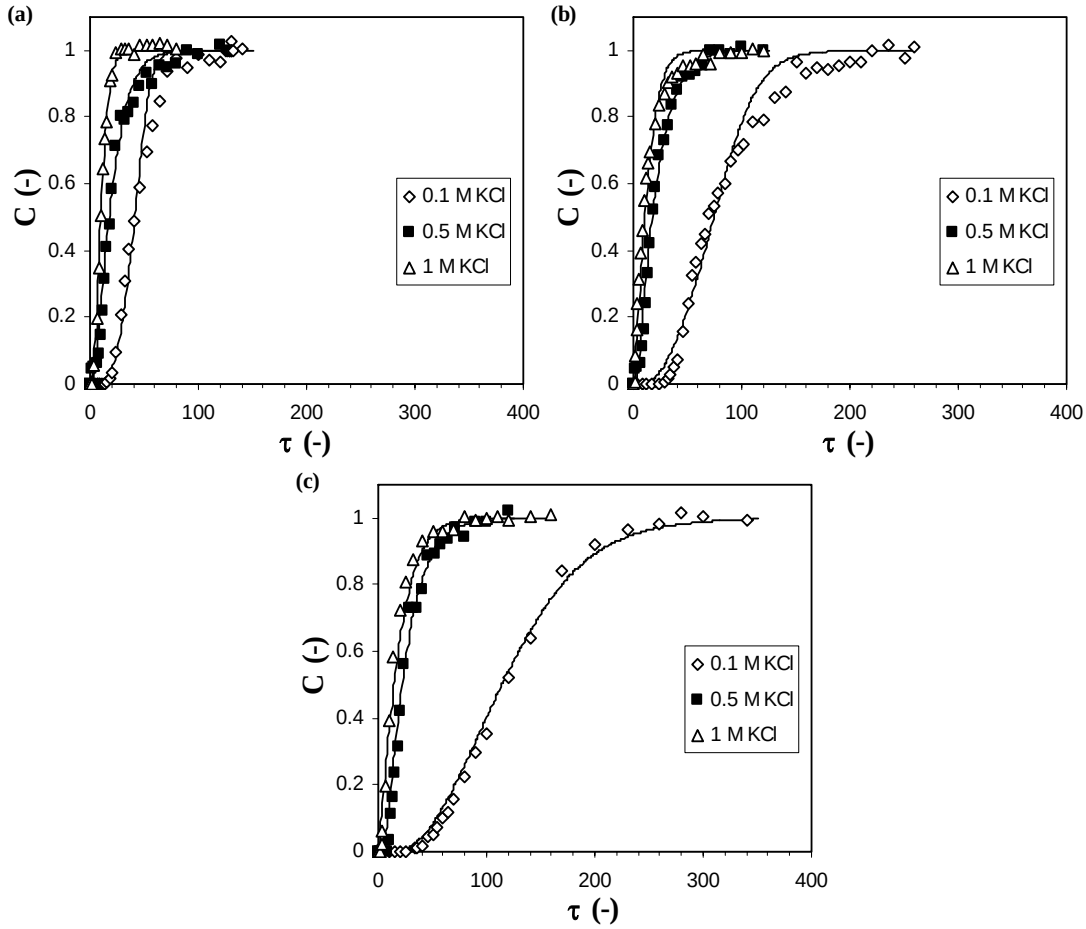

Figure 1. Experimental and calculated breakthrough curves as a function of KCl and Orange G concentrations: (a) 10^{-3} M, (b) $5 \cdot 10^{-4}$ M, and (c) $2.5 \cdot 10^{-4}$ M.

Three key parameters, which characterize the dynamic adsorption process, can be determined from the dimensionless variables: the axial diffusion coefficient, *D*, from Equation (8), the adsorption rate constant, k_a, from Equation (9), and the desorption rate constant, k_d, from Equation (10). It was observed that the axial diffusion coefficient was almost independent of ionic strength, being $1.30 \cdot 10^{-8} \pm 0.059 \cdot 10^{-8}$ m2/s, with a probability of 95%. Moreover, Table I shows the adsorption and desorption rate constant as a function of KCl concentration. As expected, the adsorption process was hindered (61%) and the desorption process increased (33%) with increasing the KCl concentration. This fact could be due to the increased shielding of electrostatic interactions between the dye and the membrane.

Table I. The values of the adsorption and desorption rate constants determined by the model as a function of KCl concentration.

KCl concentration (M)	**k_a ($L \cdot mol^{-1} \cdot s^{-1}$)**	**k_d (s^{-1})**
0.1	170	0.121
0.5	122	0.284
1.0	103	0.369

5. Conclusions

The proposed model for the modelling of the dynamic adsorption process through membrane adsorbers fits with strong correlation the experimental breakthrough curves of the anionic dye (Orange G). The experimental work investigated the equilibrium and the dynamics of the adsorption. The adsorption process was significantly affected by the dye and KCl concentrations, since the electrostatic repulsion between chloride and dye anions intensified the desorption rate constant and, at the same time, it reduced the adsorption rate constant. Nevertheless, the axial diffusion coefficient was independent of KCl concentration.

Acknowledgements

The authors are grateful to the Spanish Ministerio de Ciencia y Tecnología (project CTQ2005-08346-C02-01/PPQ) for funds received to carry out this study.

References

Arica, M.Y., Yilmaz, M., Yalcin, E. and Bayramoglu, G., (2004) *Journal of Chromatography B*, 805, 315.
Boi, C., Cattoli, F. and Facchini, R., (2006) *Journal of Membrane Science*, 273, 12.
Ghosh, R., (2002) *Journal of Chromatography A*, 952, 13.
Guo, W. and Ruckenstein, E., (2003) *Journal of.Membrane Science*, 211, 101.
Knudsen, H.L., Fahrner, R.L., Xu, Y., Norling, L.A. and Blank, G.S., (2001) *Journal of Chromatography A*, 907, 145.
Lan, Q.D., Bassi, A.S., Zhu, J.X. and Margaritis, A., (2001) *Chemical Engineering Journal*, 81, 179.
Lewus, R.K. and Carta, G., (1999) *AIChE Journal*, 45, 512.
Skidmore, G.L., Horstmann, B.J. and Chase, H.A., (1990) *Journal of Chromatography*, 498, 113.
Zhang, S.P. and Sun, Y., (2002) *Journal of Chromatography A*, 957, 89.
Zhang, S.P. and Sun, Y., (2002) *Journal of Chromatography A*, 964, 35.